BULLETIN OF THE EARTHQUAKE
RESEARCH INSTITUTE
Vol. 44 (1966), pp. 531-540

31. *Geothermal and Magnetic Survey off the Coast of Sumatra.*[*]

1. Presentation of Data.

By V. VACQUIER,
Scripps Institution of Oceanography,
University of California, San Diego
and P. T. TAYLOR,[**]
Department of Geophysics, Stanford University,
Stanford, California.

(Read March 22, 1966.—Received March 31, 1966.)

1. Abstract

Total magnetic intensity and terrestrial heat flow were observed along profiles off the coast of Sumatra. The topographic swell just seaward of the trench was found to have a heat flow greater than 1.5 μcal cm^{-2} sec^{-1}, as compared with a value of less than 1 μcal cm^{-2} sec^{-1} both in the deep trench and seaward of the swell. It is suggested that there might be a band of high heat flow in front of all deep-sea trenches. The magnetic anomalies trend mostly east-west and do not follow the curve of the Indonesian island arc.

2. Results

As the final contribution of the Scripps Institution of Oceanography to the International Indian Ocean Expedition, the research vessel ARGO, on her way between Colombo, Ceylon, and Singapore, observed 61 heat-flow stations along 8 profiles. The total magnetic intensity was also recorded all along the ship's track. The heat-flow values are shown in Figure 1. The tracks were chosen to verify the expectation that a high heat-flow anomaly might exist seaward of the trench. Examination of the previously existing observations near Indonesia, Japan, and South America (Lee and Uyeda, 1965) indicates that possibly this might be the case. As can be seen from Figure 1, this expectation has been con-

---

[*] Contribution from the Scripps Institution of Oceanography, University of California, San Diege. Communicated by S. Uyeda.

[**] Now with Lamont Geological Observatory, Palisades, New York.

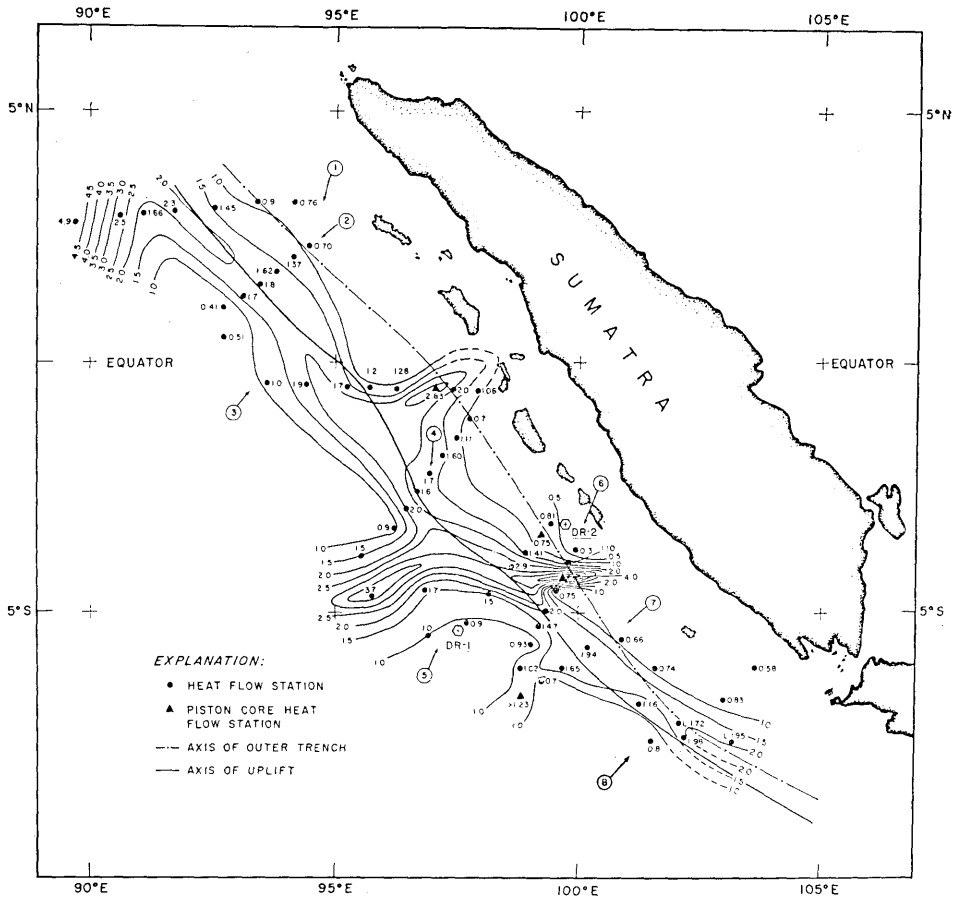

Fig. 1. Terrestrial heat flow. Contour interval is 0.5 ucal $cm^{-2} sec^{-1}$. High heat flow characterizes the topographic swell seaward of trench.

firmed. This discovery will direct the planning of future expeditions to various parts of the rim of the Pacific Ocean basin. Heat flow off the coast of North America has already been studied by Von Herzen (1964). If we find that along the remaining rim of the Pacific Ocean basin there exists a band of high heat flow, our speculations on what is going on at the edges of the oceans will have to be re-evaluated.

A detailed bathymetric map is not available for the region surveyed because the great wealth of information gathered by the ships of all participating nations in the International Indian Ocean Expeditions will take some time to assemble and will be published by others. The topographic swell, the crest of which is traced on Figure 1, can, however,

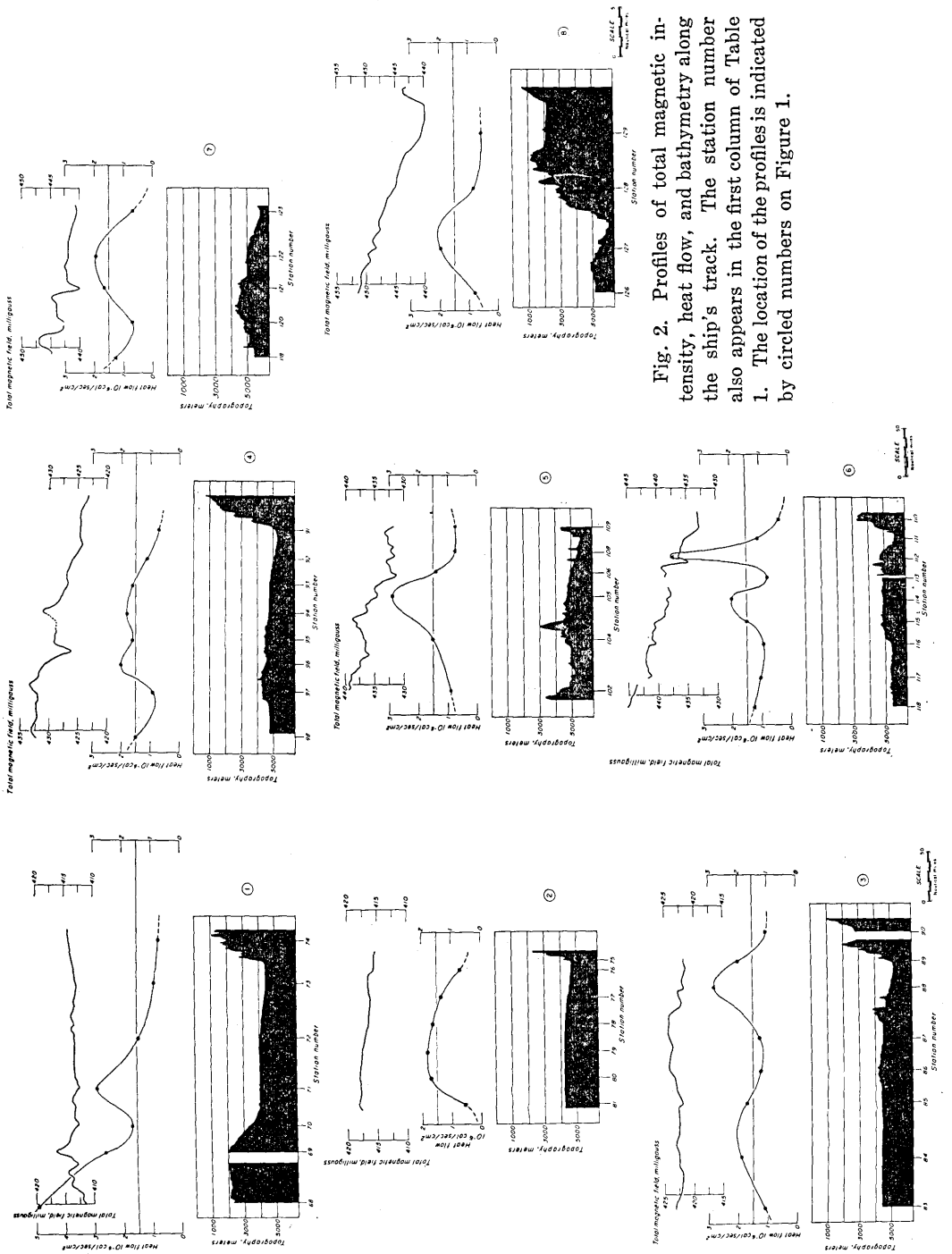

Fig. 2. Profiles of total magnetic intensity, heat flow, and bathymetry along the ship's track. The station number also appears in the first column of Table 1. The location of the profiles is indicated by circled numbers on Figure 1.

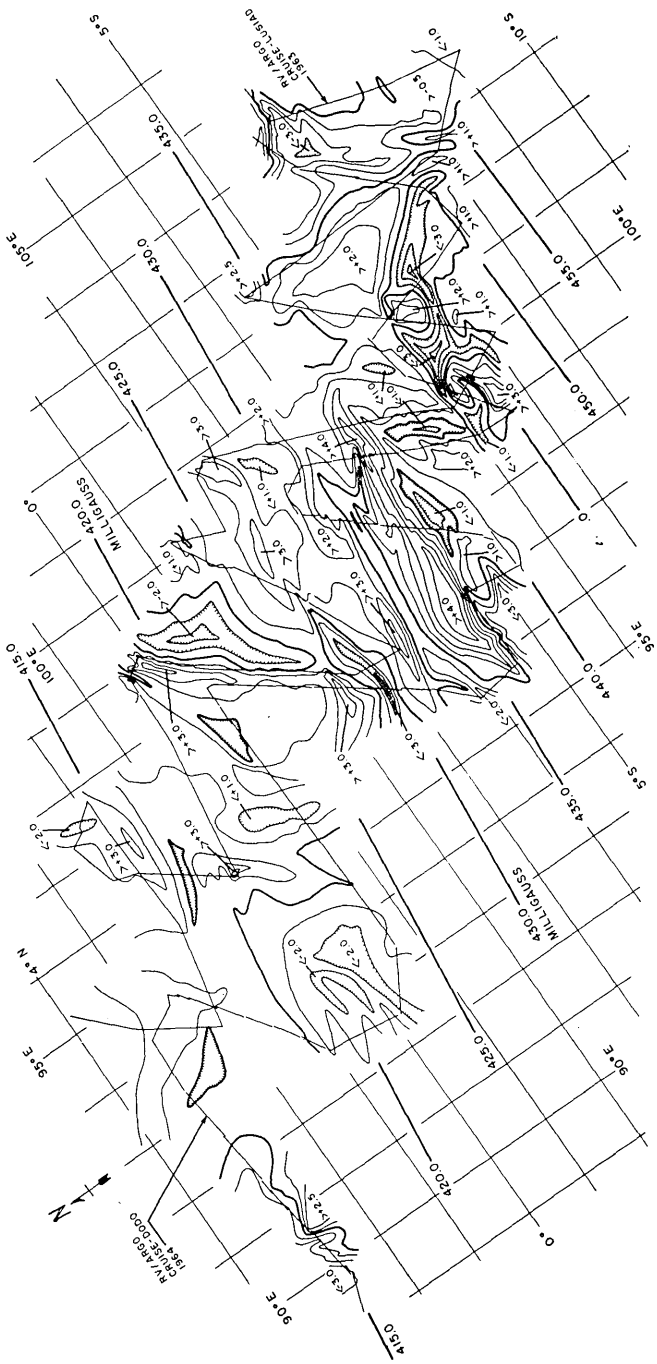

Fig. 3. Total magnetic intensity anomaly contoured with interval of 1 mgauss off the island of Sumatra. The absolute value of the total magnetic intensity in milligauss is obtained by adding the value of the contours to the regional magnetic slope indicated at the edges of the map.

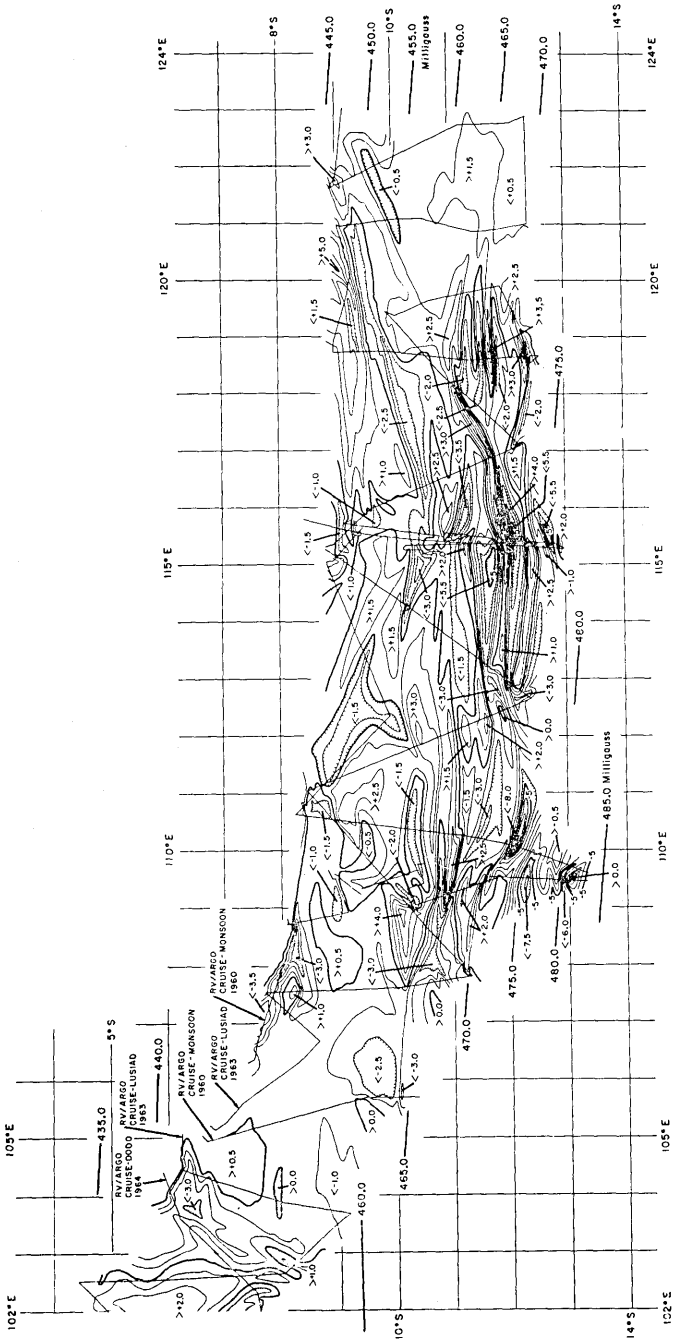

Fig. 4. Total intensity anomaly map contoured with interval of 1 mgauss off the island of Java. The absolute value of the total magnetic intensity in miligauss is obtained by adding the value of the contours to the regional magnetic slope indicated at the edges of the map.

be seen well enough on the Heezen and Tharp (1964) physiographic diagram of the Indian Ocean and on the profiles of Figure 2. The large uplift on the western part of the first profile is the "Ninety-east Ridge." High heat flow occurs on its crest. On this profile the swell seaward of the trench has almost no relief, and its axis is 120 km from the trench axis. Toward the south, the relief of the swell is more pronounced; and its axis, as well as that of the heat flow, moves, closer to the trench until they are only 40 km from it on the last profile.

Figure 1 shows a strong east-west heat-flow anomaly at 4° South that crosses the major heat-flow pattern which is parallel to the trench. This east-west anomaly also appears on the magnetic intensity map of Figure 3. North of this anomaly the magnetic field is relatively smoother than south of it. This east-west anomaly may represent a volcanic fracture zone. An attempt was made to contour the sparse magnetic data south of Java from Expedition Monsoon (see Figure 4). This map indicates that the magnetic anomalies have not changed their east-west trend and are running mostly parallel to the Java coast. It is possible that the magnetic anomalies in the ocean are unaffected by the island arc. Similar results are found for the magnetic anomalies off the coast of Japan, east to Tokyo, where the magnetic trend is parallel to the pattern found off the Kurile trench (Uyeda *et al.*, 1964).

The location of the two rock dredges made during the survey are labeled DR 1 and DR 2 in Figures 1 and 2. Weathered vescicular basalt was found at DR 1 westward of the trench, and a sandy shale was dredged from the eastern slope of the trench.

3. Experimental details

All but 4 stations were taken with the Von Herzen short temperature gradient probe previously described (Von Herzen and Uyeda, 1963). The others were observed with a piston corer probe carrying outrigger sensors (Gerard, *et al.*, 1962). Intermittently, gravity and piston cores were taken and the termal conductivity measured on shipboard by the needle-probe method of Von Herzen and Maxwell (1959). All of the data are listed in Table 1. Stations L 1.72 and L 1.95 in Figure 1 were previously taken by the Lamont Geological Observatory and therefore are not listed in Table 1.

The sediments encountered in the area of the survey were often a hard blue clay which accounts for the more than usual number of partial

Table 1. Summary of new heat flow data off Sumatra, Expedition DODO

Heat Flow Sta. No.	Lat.	Long.	Thermal Grad. (10^{-3}° C/cm)	Thermal Cond. (10^{-3} cal /cm sec°C)	Heat Flow (10^{-6} cal /cm^2 sec)	Depth (meters)
65	04-23N	84-41E	0.59	2.07	1.22	4170
66	03-23N	86-34E	0.60	(2.07)	1.24	4152
67	02-58N	88-49E	0.61	2.06	1.25	4020
68	02-42N	89-44E	2.38	(2.06)	4.9	2360
69	02-51N	90-36E	1.21	(2.06)	2.5	2060
70	02-56N	90-03E	0.81	(2.04)	1.66	3475
71	02-58N	91-41E	1.13	2.04	2.3	4103
72	03-04N	92-31E	0.69	2.11	1.45	4200
73	03-10N	93-22E	0.43	(2.11)	0.9	4570
74	03-09N	94-07E	0.30	2.55	0.76	2145
—						
76	02-20N	94-27E	0.25	2.80	0.70	4801
77	02-04N	94-07E	0.57	2.40	1.37	4620
78	01-49N	93-47E	0.75	2.15	1.62	4398
79	01-33N	93-27E	0.84	(2.15)	1.8	4320
80	01-18N	93-06E	0.79	(2.15)	1.7	4330
81	01-05N	92-42E	0.25	(1.63)	0.41	4390
82	00-30S	92-42E	0.31	1.63	0.51	4510
83	00-25S	93-36E	0.61	(1.63)	1.0	4550
84	00-27S	94-24E	1.16	(1.63)	1.9	4530
85	00-29S	95-15E	1.04	(1.63)	1.7	4690
86	00-30S	95-42E	0.61	(2.0)	1.2	4279
87	00-31S	96-14E	0.64	(2.0)	1.28	4634
88*	00-32S	97-02E	1.25	2.26	2.83	5125
89	00-33S	97-24E	0.88	(2.26)	2.0	5190
90	00-34S	97-54E	0.59	1.79	1.06	2870
91	01-08S	97-45E	0.39	(1.79)	0.7	5360
92	01-31S	97-28E	0.62	(1.79)	1.11	5232
93	01-53S	97-10E	0.83	1.92	1.60	4940
94	02-14S	96-55E	0.88	(1.92)	1.7	4890
95	02-35S	96-40E	0.83	(1.92)	1.6	4611
96	02-56S	96-26E	1.09	1.83	2.0	4610
97	03-19S	96-10E	0.49	(1.83)	0.9	4425
98	03-52S	95-38E	0.82	(1.83)	1.5	4920
99	04-41S	95-45E	2.02	(1.83)	3.7	4840
100	04-34S	96-49E	0.93	(1.83)	1.7	5342

(to be continued)

(continued)

Heat Flow Sta. No.	Lat.	Long.	Thermal Grad. (10^{-3}° C/cm)	Thermal Cond. (10^{-3} cal /cm² sec)	Heat Flow (10^{-6} cal /cm² sec)	Depth (meters)
101	05-27S	96-55E	0.55	(1.83)	1.0	4676
102	05-12S	97-41E	0.48	(1.89)	0.9	4360
—						
104	04-38S	98-09E	0.79	(1.89)	1.5	4758
105	04-04S	98-37E	1.53	1.89	2.9	4879
106	03-48S	98-53E	0.75	1.90	1.41	5280
108*	03-27S	99-13E	0.34	2.20	0.75	5715
109	03-13S	99-25E	0.37	(2.20)	0.81	4570
110	03-44S	99-56E	0.14	(2.20)	0.3	3445
111	03-59S	99-48E	0.50	2.20	1.10	5860
112*	04-18S	99-40E	2.25	1.91	4.0	4890
113	04-38S	99-29E	0.39	(1.91)	0.75	5015
114	04-57S	99-20E	1.05	(1.91)	2.0	5115
115	05-18S	99-11E	0.77	(1.91)	1.47	5006
116	05-39S	99-02E	0.49	(1.91)	0.93	5572
117	06-07S	98-50E	0.53	(1.91)	1.02	5500
118*	06-41S	98-50E	0.68	1.81	>1.23	5640
—						
120	06-22S	99-15E	0.39	(1.81)	0.7	4974
121	06-06S	99-40E	0.91	(1.81)	1.65	4755
122	05-43S	100-11E	1.07	(1.81)	1.94	5180
123	05-33S	100-54E	0.36	(1.81)	0.66	6040
124	06-08S	101-05E	0.46	(1.61)	0.74	5660
125	06-53S	101-15E	0.72	1.61	1.16	5460
126	07-40S	101-33E	0.50	(1.61)	0.8	5315
127	07-31S	102-17E	1.23	(1.61)	1.98	5660
128	06-50S	102-58E	0.49	1.68	0.83	2760
129	06-11S	103-36E	0.34	(1.68)	0.58	2250

The heat flow values with asterisks indicate that they were obtained with the Ewing instrument. The thermal conductivity values in parentheses are those values obtained at stations other than the one at which the heat flow was being computed. Heat flow values with one figure after the decimal point indicate that these values were obtained from partial penetration of the thermal probe.

penetrations by the probe. The amount of penetration can be estimated from the bend of the probe. In most of the heat-flow measurements, a hard steel probe was used. This hard probe does not bend reliably

on pull-out. It was threfore necessary to find another method for estimating the depth of penetration of the probe. This was accomplished by taping to the probe 3 miniature core barrels 80, 110, and 150 cm from the end of the probe staff. Counting full penetration, which is established with the large (Phleger) core barrel at the bottom of the instrument case had caught some sediment, this method gave us 4 reference points for estimating penetration. The shape of the small mud catches was such that they could not be filled with mud by dragging the instrument along the sea floor.

4. Acknowledgments

We are indebted to Dr. R. P. Von Herzen for the development and construction of the instruments we used; to Messrs. F. S. Dixon, J. G. Sclater, and R. E. Warren for assistance at sea. Mr. G. Gassaway constructed the illustrations. This work was supported by contracts Nonr 2216 (05) and NSF-G22255.

References

GERARD, R., M. G. LANGSETH, Jr., and M. EWING. Thermal gradient measurements in the water and bottom sediment of the Western Atlantic, *J. Geophys. Res.*, **67**, 785-803, 1962.

HEEZEN, B. C., and M. THARP. Physiographic diagram of the Indian Ocean, *Geological Society of America*, New York, 1964.

LEE, W. H. K., and S. UYEDA. Review of heat-flow data, Chapter 6 in *Terrestrial Heat Flow*, edited by W. H. K. Lee, Geophysical Monograph No. 8, American Geophysical Union, pp. 87-190, 1965.

UYEDA, S., T. SATO, M. YASUI, T. YABU, T. WATANABE, K. KAWADA, and Y. HAGIWARA. Report on geomagnetic survey in the northwestern Pacific during JEDS-VI, JEDS-VII, and JEDS-VIII Cruises, *Bull. Earthq. Res. Inst., Univ. Tokyo*, **42**, 555-570, 1964.

Von HERZEN, R. P. Ocean-floor heat-flow measurements west of the United States and Baja California, *Marine Geo.*, **1**, 225-239, 1964.

Von HERZEN, R. P., and A. E. MAXWELL. The measurement of thermal conductivity of deep-sea sediments by a needle-probe method, *J. Geophys. Res.*, **64**, 1557-1563, 1959.

Von HERZEN, R. P., and S. UYEDA. Heat flow through the eastern Pacific Ocean floor, *J. Geophys. Res.*, **68**, 4219-4250, 1963.

31. スマトラ島沖の地熱及び地磁気調査

1. 観 測 結 果

カリフォルニア大学 スクリプス海洋研究所 V. VACQUIER
スタンフォード大学 地球物理学教室 P. T. TAYLOR

スマトラ島沖の印度洋において，地磁気全磁力および，地殻熱流量の調査が行なわれた．海溝沖合の海底台地では熱流量は，1.5 μcal/cm^2 sec より大きく，海溝および，台地より海洋側での低い値(<1 μcal/cm^2 sec) と対照的であることが判つた．このような帯状分布は，海溝地域一般にみられるものの如くである．地磁気異常帯の向きは主として東西であつて，インドネシア島弧の屈曲に沿うてはいない．